water

MDPI

*Article*

# An Evaluation of a New Scheme for Determination of Irrigation Depths in the Egyptian Nile Delta

**Hassan M. Abd El Baki and Haruyuki Fujimaki ***

Arid Land Research Center, Tottori University, Tottori 680-0001, Japan; hassan.wat2@yahoo.com
* Correspondence: fujimaki@tottori-u.ac.jp; Tel.: +81-857-21-7040; Fax: +81-857-29-6199

**Abstract:** Innovative irrigation techniques should be implemented to improve irrigation management in dryland countries. In this regard, a new scheme, that uses three sets of irrigation depth and numerically simulated cumulative transpiration, was evaluated in the Egyptian Nile delta in 2020. Presuming that water is volumetrically priced, the proposed scheme can maximize net incomes at optimum irrigation depths considering quantitative weather forecasts. A field experiment was carried out with a randomized complete block design using a major crop, maize, to assess the feasibility of the proposed scheme in comparison to a sensor-based irrigation method under conditions of dry climate and clay loamy soil. The proposed scheme could increase the gross net income of farmers and conserve irrigation by 21% and 35%, respectively, compared to a sensor-based irrigation method, although the yield and its components were almost the same with no significant statistical differences. The model could accurately simulate soil water content in the topsoil layers with a RMSE of 0.02 $cm^3$ $cm^{-3}$. The proposed scheme could be a useful tool to spare the costs of expensive soil monitoring sensors while saving water and improving net income.

**Keywords:** weather forecast; dryland; dielectric sensors; net income; optimization; drought



**Citation:** Abd El Baki, H.M.; Fujimaki, H. An Evaluation of a New Scheme for Determination of Irrigation Depths in the Egyptian Nile Delta. *Water* **2021**, *13*, 2181. https://doi.org/10.3390/w13162181

Academic Editors: Vinay Nangia and Anurag Saxena

Received: 4 June 2021
Accepted: 8 August 2021
Published: 9 August 2021



## 1. Introduction

Irrigation management is a crucial practice in arid regions experiencing water shortage. Egypt is one of those countries, where agriculture is mostly dependent on the Nile River water. The rapid growth of the Egyptian population is exacerbating the stress on the water supply. According to the Ministry of water resources and irrigation of Egypt, the total water supply is 59.52 BCM/year, while the total current water demand is 80 BCM/year. Moreover, the per capita share of renewable water resources is forecasted to reach 250 $m^3$/year in 2050 [1]. The deficiency of available water resources evokes the development of new practical techniques adaptive for farmers to improve irrigation management.

To alleviate the stress of limited water resources, the deficit irrigation (DI) technique has been introduced to either save water or increase water use efficiency (WUE). DI is a practice whereby water is applied at less than crop water requirements (CWR) [2]. It necessitates precise data on crop response to drought stress throughout the growing season [3]. Much published research has shown the efficacy of DI in terms of water use and WUE without substantial effects on final yield [4–6]. In contrast, other studies have shown that DI has a negative impact on WUE. For example, Bell et al. [7] compared managed deficit irrigation (MDI), which aims to optimize both yield and WUE by linking CWR to productive stages, to DI, and to full irrigation (FI). They observed that both MDI and DI significantly reduced the WUE compared with FI. It is not always the case that DI improves WUE. If maximizing WUE is the primary target, farmers may not obtain sufficient yield to sustain their living. Thus, the primary target of irrigation is to maximize farmers' net income ($I_n$) rather than WUE [8].

To improve irrigation management to precisely meet with CWR, affordable soil, plant, and weather sensors have been developed. Several researchers showed the effectiveness

of soil water monitoring on irrigation control [9–11]. According to Hedley et al. [12] and Adeyemi et al. [13], dielectric soil moisture sensors are commonly used to monitor the spatiotemporal soil water dynamics on the field scale. However, these sensors are initially costly, and therefore it is difficult for farmers living in developing countries in arid regions like Egypt to obtain them. It also requires proper calibration at each site.

With the availability of meteorological variables such as solar radiation, wind speed, relative humidity, temperature and rainfall, capital-intensive sophisticated soil moisture sensors and dataloggers have been able to be replaced by numerical simulation models, that can simulate the crop response to irrigation. Li et al. [14] used a simulation–optimization model to optimize irrigation scheduling for maize crop in arid oasis in China. Pereira et al. [15] used soil water balance models to determine both crop water requirements and irrigation scheduling using the FAO56 method [16] and the dual crop coefficient. Several researchers used the HYDRUS model [17] to simulate soil water and salinity distributions under different irrigation systems such as Selim et al. [18] and Noshadi et al. [19], or to simulate evapotranspiration (ET) [20].

To avoid the drawbacks of sensors or other techniques mentioned above, the combination between quantitative weather forecast (WF) and numerical simulations considering crop response to drought and salinity stresses can be an effective means to improve irrigation management. Recently, free accessible online WF with fair accuracy was used to optimize irrigation scheduling [21]. In addition to free and easy access to weather forecast, computers with high-speed CPU are becoming affordable even for farmers in low-income countries. Optimization of irrigation depths that maximize $I_n$ using WF and numerical simulation has been studied by several researchers. Some of them optimized irrigation depths corresponding to the maximal seasonal net income using a combination between genetic algorithms and the SWAP model [22–24]. However, they used simplified water-yield relationships in their calculations. The cumulative transpiration simulated by the WASH 2D model [8] using the past weather and WF was used to determine the irrigation depths that maximize net income at each irrigation event [8,25–28]. Such studies are based on the concept of volumetric water pricing to motivate farmers to save irrigation. Still, the validation studies have been limited to the combination of a humid climate and a sandy soil.

This research was conducted with the perspective of Egypt's prevailing water scarcity, particularly during the dry months, and because we could not identify studies that integrated irrigation depth determination, net income maximization, and weather forecast utilization by considering volumetric water pricing and crop response to drought stress. The study was carried out in farmland in the north-western part of the Nile Delta, using a major crop, maize. The main objective, therefore, was to investigate and compare the effectiveness of the proposed scheme using numerical simulation of water flow in the soil–water–atmosphere system using the WASH 2D model [8] for the sensor-based irrigation method in terms of irrigation depths and net incomes under conditions of dryland and clay loam.

## 2. Materials and Methods

### *2.1. Scheme for Determining Irrigation Depth*

#### 2.1.1. Net Income

To achieve optimal use of water that contributes to farmers' economic benefits, $I_n$ (\$ ha$^{-1}$) is calculated according to Fujimaki et al. [8] as:

$$I_n = P_c \varepsilon \tau_i k_i - P_w W - C_{ot}, \quad (1)$$

The first term in Equation (1) ($P_c \varepsilon \tau_i k_i$) represents the total income that a farmer may obtain at each irrigation event, where $P_c$ is the producer's price of crop (\$ kg$^{-1}$ dry matter (DM)); $\varepsilon$ is the transpiration efficiency of the crop (produced dry matter (kg ha$^{-1}$) divided by cumulative transpiration (kg ha$^{-1}$)); $\tau_i$ is the cumulative transpiration between two irrigation events (1 mm = 10,000 kg ha$^{-1}$); and $k_i$ is the income correction factor. The

second term ($P_w W$) and the third term ($C_{ot}$) in Equation (2), represent the costs spent for producing the crop, where $P_w$ is the price of water (\$ kg$^{-1}$); $W$ is the irrigation depth (1 mm = 10,000 kg ha$^{-1}$); and $C_{ot}$ is other costs (e.g., fertilizer, labor, etc.) (\$ ha$^{-1}$). Note that the $\tau_i$ in the initial crop stage is far lower than later growth stages. Therefore, $k_i$ was used to avoid possible underestimation of $I_n$, and it was calculated as [8]:

$$k_i = \frac{\bar{k}_{cb}}{k_{cb}} = \frac{\int k_{cb} d\tau}{\tau_f k_{cb}}, \quad (2)$$

where $\bar{k}_{cb}$ is the average value of the basal crop coefficient, $k_{cb}$ for a given growth period; and $\tau_f$ is the expected cumulative transpiration at the end of this period.

2.1.2. Optimal Irrigation Depth

Optimal irrigation management necessitates precise data on crop response to drought stress throughout the growing season. Since the transpiration is directly linked to the crop growth and productivity, $\tau_i$ is described with a non-linear function of $W$:

$$\tau_i = \int T_r dt = a_t[1 - \exp(b_t W)] + \tau_0, \quad (3)$$

where $T_r$ is the transpiration rate (cm s$^{-1}$), $a_t$ and $b_t$ are fitting parameters; and $\tau_0$ is the initial cumulative transpiration. The optimal irrigation depth corresponding to maximum $I_n$ ($I_{n_{max}}$) is achieved when the first derivative of Equation (1) with regard to W becomes zero as follows:

$$\frac{dI_n}{dW} = -P_c \varepsilon k_i a_t b_t \exp(b_t W) - P_w = 0, \quad (4)$$

Then, the optimal irrigation depth is determined as:

$$W = \frac{1}{b_t} \ln\left(-\frac{P_w}{P_c \varepsilon k_i a_t b_t}\right), \quad (5)$$

To solve Equation (5), $a_t$ and $b_t$ were determined at two-point combination sets of $\tau_i$. and $W$ as shown in Figure 1 as:

$$\tau_{max} = a_t[1 - \exp(b_t W_{max})] + \tau_{0,} \quad (6)$$

$$\tau_{mid} = a_t[1 - \exp(b_t W_{mid})] + \tau_0, \quad (7)$$

Solving Equations (6) and (7) together gives

$$a_t = \frac{\tau_{max} - \tau_{mid}}{(\exp(b_t W_{mid}) - \exp(b_t W_{max}))} \quad (8)$$

Therefore, $a_t$ is determined when:

$$\frac{\tau_{max} - \tau_{mid}}{(\exp(b_t W_{mid}) - \exp(b_t W_{max}))} - \frac{\tau_{max} - \tau_0}{(1 - \exp(b_t W_{max}))} = 0. \quad (9)$$

The value of $b_t$ can be easily obtained using the bisection method.

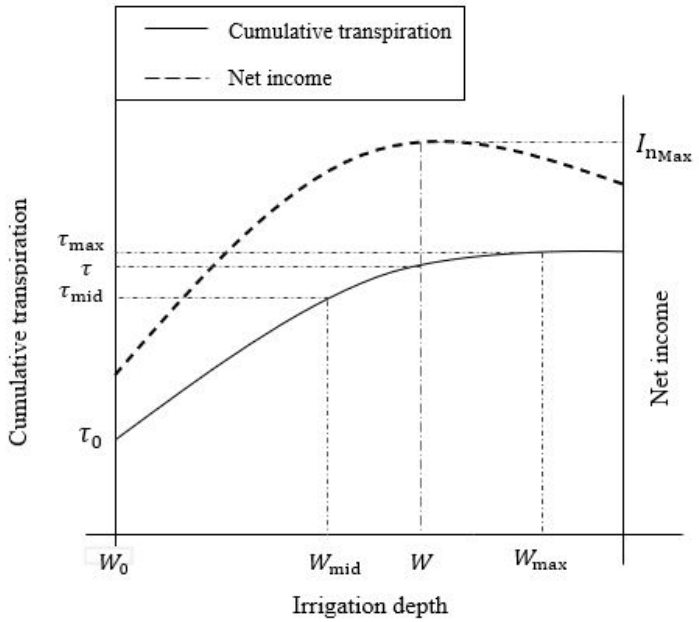


**Figure 1.** Schematic diagram of irrigation depth determination that maximizes net income using the proposed scheme [8].

### *2.2. The Simulation Model*

The scheme described above was incorporated into a numerical model, WASH_2D, which solves the governing equations of the two-dimensional flow of water, solutes, and heat in soils. The model can partition the evapotranspiration into transpiration and evaporation. It also includes a module for simulating plant root water uptake. Thus, the actual transpiration rate, $T_a$ can be estimated by integrating the water uptake over the plant rootzone. The potential transpiration, $T_p$ was calculated as:

$$T_p = E_p k_{cb}, \tag{10}$$

where $E_p$ is the reference evapotranspiration (cm $s^{-1}$), calculated by the Penman–Monteith equation [16] and $k_{cb}$ is the basal crop coefficient, which is expressed as a function of cumulative transpiration as:

$$k_{cb} = a_{kc}[1 - \exp(b_{kc}\tau)] + c_{kc} - d_{kc}\tau^{e_{kc}}, \tag{11}$$

where $a_{kc}$, $b_{kc}$, $c_{kc}$, $d_{kc,}$ and $e_{kc}$ are fitting parameters. The parameter values in Equation (5) were derived from fittings to those reported by Allen et al. [16]. Instead of the commonly used function of $k_{cb}$ in terms of days after planting, we related $k_{cb}$ to the cumulative transpiration so that the model could express the plant growth more dynamically to both drought and salinity stresses.

### *2.3. The Simulation Procedure*

The optimal irrigation depth is achieved by performing two major steps at each irrigation interval as shown in Figure 2. In this study, the irrigation interval was set at three days. In the morning of an irrigation day ($t_0$), the update run was performed using the records of the actual weather, irrigation, and cumulative transpiration to estimate the initial condition for the past 72 h. Then, both the results of the update run and quantitative WF data were used in the optimization run to determine the irrigation depth that maximizes the $I_n$ for the next 72 h.

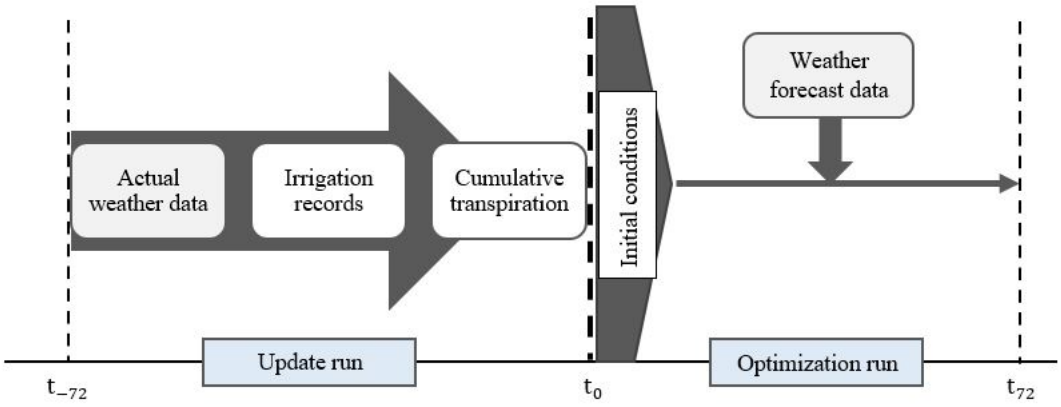


**Figure 2.** The routine simulation procedure in the WASH 2D model to determine irrigation depths using the proposed numerical scheme (two major runs to optimize irrigation depths: update and optimization).

### *2.4. Field Experiment*

A field experiment was carried out in a farmland in the north-western part of the Nile Delta, Kafrelshiekh governorate, Egypt in 2020 (31°12′34.6″ N, 30°34′6.3″ E). The experimental field was located away from the rice-growing area to avoid the effect of rising water table to water balance. The groundwater table was below 1 m throughout the experimental period. Two treatments were established: (1) the proposed scheme (A), and (2) sensor-based irrigation (B). Each treatment had three replicates. The length of each replicate was 2 m. The irrigation was applied through a drip irrigation system with laterals and emitters spaced at 80 cm and 30 cm, respectively. Each replicate had five drip tubes. The discharge rate of each emitter was 2 L $h^{-1}$. The treatments and replicates were set in a randomized complete block design. Two dielectric moisture sensors, 10HS (METER Inc., Pullman, Washington, USA) were used to operate the irrigation for treatment B, when the average value of the two sensors dropped below 0.25. Another dielectric moisture, salinity, and temperature sensor, 5TE (METER Inc., Pullman, Washington, USA) was used to monitor volumetric water content (VWC) in treatment A in two dimensions (x = 0, horizontal distance from the drip tube and z = 5 cm, soil depth). Both sensors were calibrated for the soil as shown in Figure 3. The root mean square error (RMSE) was calculated between the observed calibrated values of the 5TE sensor and simulated ones obtained from the numerical simulations from 3 July to 18 July to assess the feasibility of the WASH 2D model for simulating soil water flow.

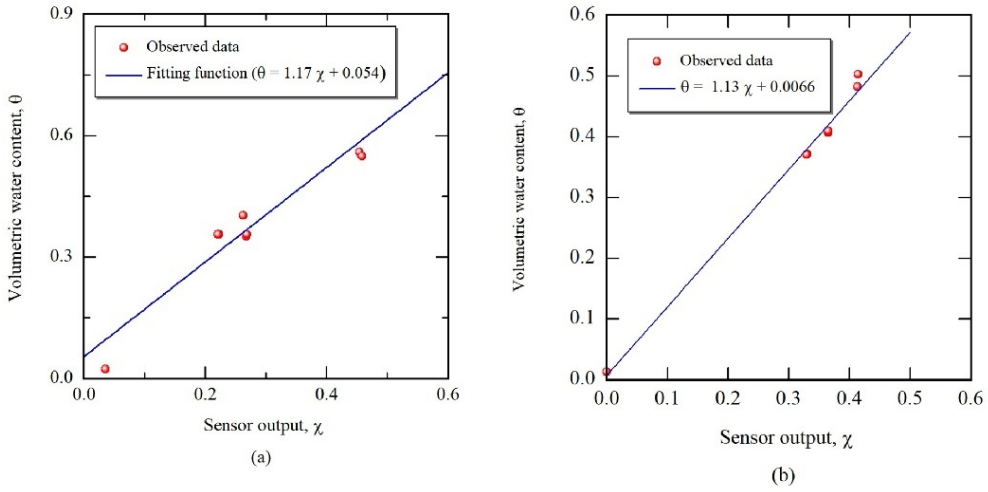


**Figure 3.** Calibration functions for (**a**) 5TE and (**b**) 10 HS in a clay loam soil in Fuwa, Egypt.

The soil was a clay loam, and its hydraulic properties were measured in the laboratory using an evaporation method [29] as shown in Figure 4. Other parameters such as solute transport and thermal conductivity were taken from similar soil in Zankalon, Sharkia, Egypt [30] and can be acquired online (http://www.alrc.tottori-u.ac.jp/fujimaki/download/WASH_2D/, accessed on 8 August 2021).

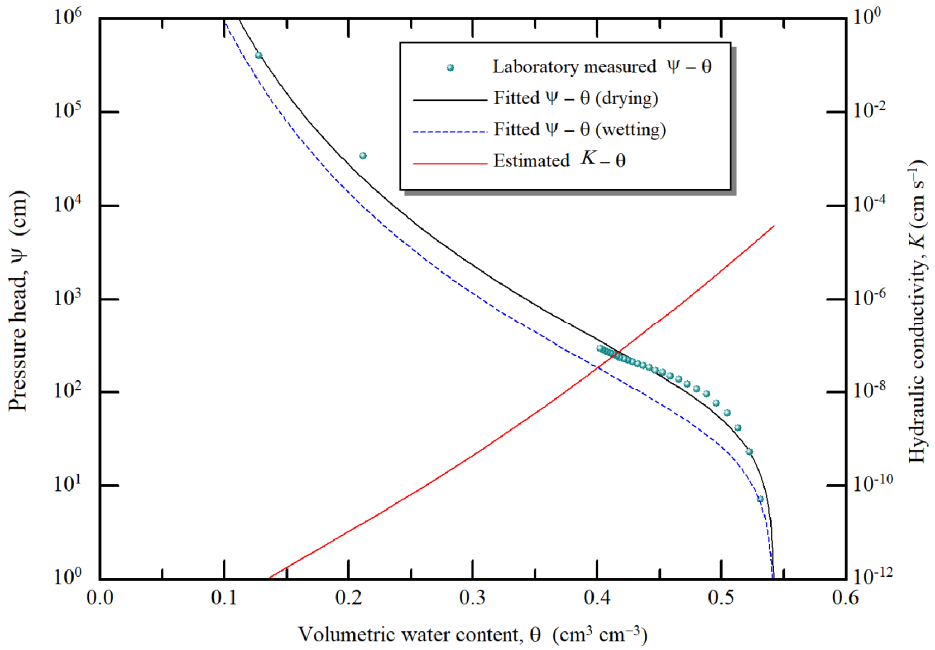


**Figure 4.** Soil hydraulic properties for clay loam, Fuwa, Egypt (the data obtained using the Fujimaki and Yanagawa [29] method).

Since the weather stations were not available, both weather and WF data were obtained from the TimeAndDate website [31] assuming the weather forecast to be accurate in the dry climate as indicated by Cai et al. [32]. Note that the WF data obtained from that link was forecast by the atmospheric general circulation models (AGCMs) for the nearest location (Al-Nozha airport, Alexandria, Egypt), which is 60 km away from the experiment field.

Maize, a popular summer crop for Egyptian Nile delta farmers, (*Zea mays* L. cv. Giza 131), was sown at a rate of one plant per emitter on 6 June 2020. All perspective agricultural treatments were performed according to the general guidelines (e.g., thinning (17 June), pesticide application to control green cotton worm using lanate 90% SP (21 and 30 June), and weed control along the plant growth). Solid fertilizers: urea and the fertilizer (N = 20%, $P_2O_5$ = 20%, $K_2O$ = 20%) were applied at total rates: 300 kg $ha^{-1}$ and 400 kg $ha^{-1}$, respectively as recommended by El-Tantawy et al. [33]. Since the WASH 2D model simulates only one solute, we simulated the fate of nitrate uptake and leaching for both treatments throughout the growing season as it is the most determinant factor for crop growth. The crop coefficient parameters were derived by setting the average evapotranspiration during initial, development, mid and late stages as 3, 4, 5, 5 mm $d^{-1}$, respectively (Figure 5). Other parameter values used to describe plant properties can be found in (http://www.alrc.tottori-u.ac.jp/fujimaki/download/WASH_2D/, accessed on 8 August 2021).

The producer price in Equation (1) for maize was set at 0.1 \$ $kg^{-1}$ DM and the price of water was set as 0.0001 \$ $kg^{-1}$ [34]. Transpiration efficiency was set at 0.003. Plant height (PH) (cm) and leaf area (leaf length (cm) × leaf width (cm) × shape factor (0.77)) were measured using a graduated ruler. Leaf area index (LAI) (leaf area/plant projected area) leaves number (LN), and PH were observed every two weeks along the growing season to accurately measure the differences between the two treatments. Maize was harvested on 7 September 2020. Five plants from each replicate were randomly selected and used

to estimate yield and its components (stem DM (g), leaves DM (g), ear weight (g), ear diameter (cm), ear length (cm), cop weight (g), number of kernels per row, numbers of kernels per ear, weight of kernels per ear (g), and weight of 100 grains per ear (g)). A schematic diagram for the measured ear components is shown in Figure 6. The plant dry matter was observed using an oven whose temperature was set at 65 °C. The data was statistically analyzed with a randomized complete block design based on two-way ANOVA with replication using MS-Excel 2016 to evaluate significant differences between the two treatments.

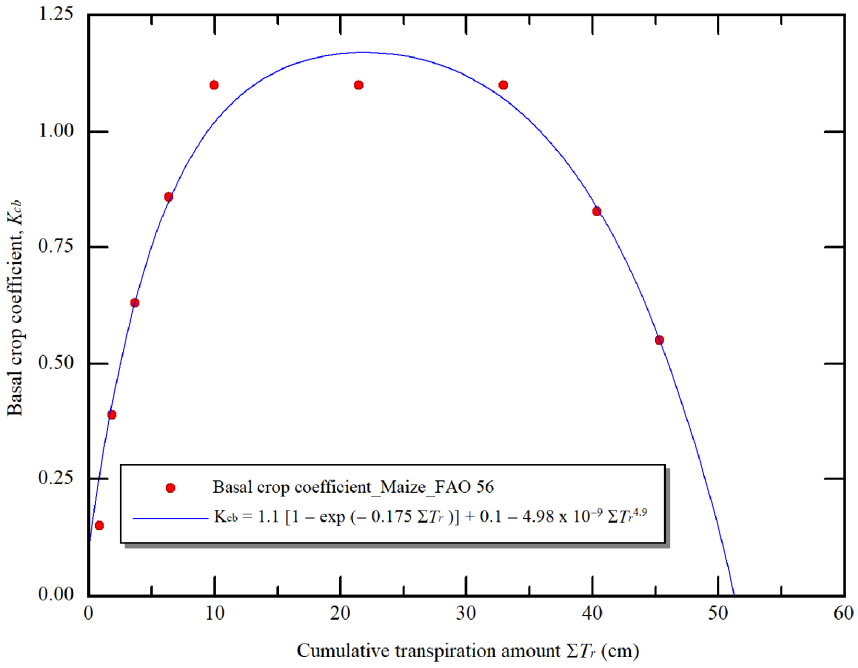


**Figure 5.** Basal crop coefficient function used by the WASH 2D model for maize crop (the function parameters were acquired from fitness to the $k_{cb}$ values reported by Allen et al. [16].

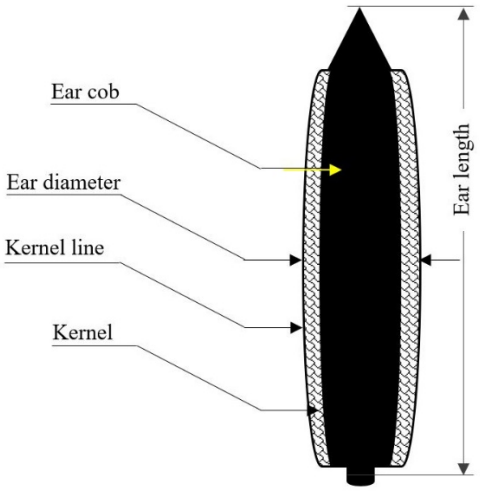


**Figure 6.** A schematic diagram for ear measured components.

## 3. Results and Discussion

### 3.1. Plant Growth and Yield Components

The comparison of plant growth such as LAI, LN, and PH was performed to assess the feasibility of the proposed scheme versus sensor-based irrigation, as shown in Figure 6. LAI increased at the same rate in both treatments, and the plant leaves began to senesce after 5 August (Figure 7a). LN increased at the same rate in both treatments until 22 July, then remained constant during the flowering stage from 22 July to 5 August, before starting to decline during the filling stage after 5 August (Figure 7b). In both treatments, the PH reached the maximum value on 5 August, and then remained nearly constant throughout the filling stage (Figure 7c). At harvest, the values of total non-grain biomass obtained for the A and B treatments were 26.6 Mg $ha^{-1}$ and 29.0 Mg $ha^{-1}$, respectively. These findings matched those of Infante et al. [35], who reported that temperate maize non-grain biomass ranges from 26 to 31 Mg $ha^{-1}$. One possible explanation for the differences in non-grain biomass is that nitrate uptake in treatment B was slightly higher than in treatment A at the same rate of nitrate leaching as shown in Figure 8. Yield components for both treatments are listed in Table 1. There were no significant differences in whole yield components between the two treatments. The weight of stem dry matter in treatment B had higher values than that of treatment A. This resulted in higher final total biomass for treatment B compared to treatment A. Despite the total weight of ears per plant being nearly the same, the weight of kernels per plant in treatment A was higher than in treatment B. This is because in treatment A, many plants tended to produce two ears compared to treatment B. Therefore, total grain yields for treatments A and B were nearly the same at 14.0 Mg $ha^{-1}$ and 13.9 Mg $ha^{-1}$, respectively (Figure 9).

### 3.2. Net Income, Grain Yield, and Applied Irrigation

The comparison between net income, grain yield, and applied water between the two treatments is shown in Figure 9. A 35% reduction in applied water caused treatment A to achieve a higher net income by around 20% of treatment B with nearly the same grain yields. This result in parallel with other results reported by Abd El Baki et al. [25–27] demonstrates the feasibility of the proposed scheme to enhance net income. In the Nile delta where the downstream farmers are often unable to obtain sufficient water due to the upstream farmers' behavior towards full or over irrigation, water inequity and conflicts have always existed [36]. Under the current water scarcity situation, it is worthwhile considering volumetric water pricing to give farmers an incentive to save water. Bozorg-Haddad et al. [37] found that low water prices have no effect on water use compared to non-priced water. The result of this study implies that even at low water price (0.1 \$ $m^{-3}$), the proposed scheme could increase farmers' net income compared to sensor-based irrigation.

### 3.3. Soil Water Content

The accuracy of the WASH 2D model in terms of water flow simulation is illustrated in Figure 10.

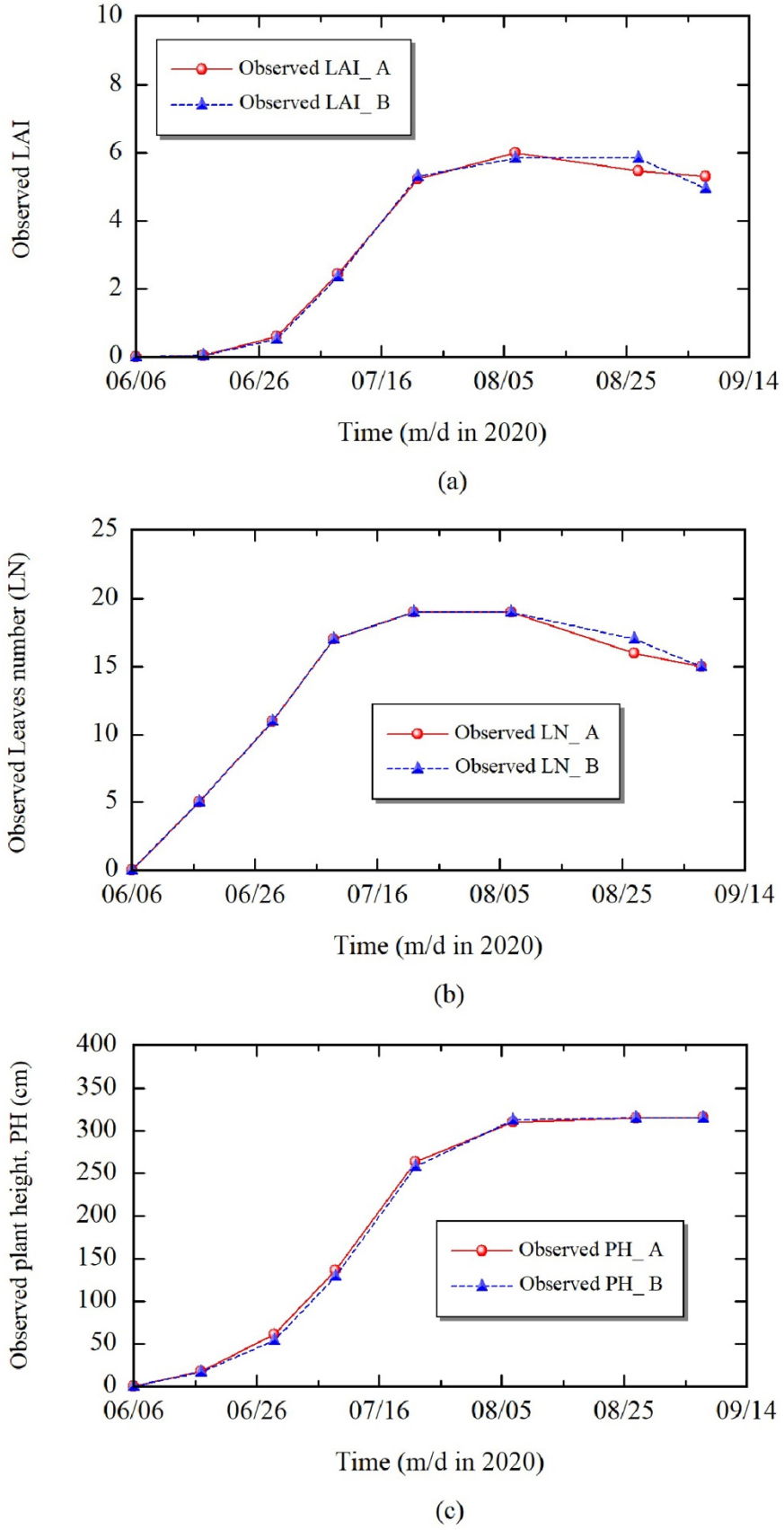


**Figure 7.** Evolution of (**a**) leaf area index, (**b**) leaves number and (**c**) plant height throughout the growing season. (A donates the proposed scheme, while B donates the sensor-based irrigation method).

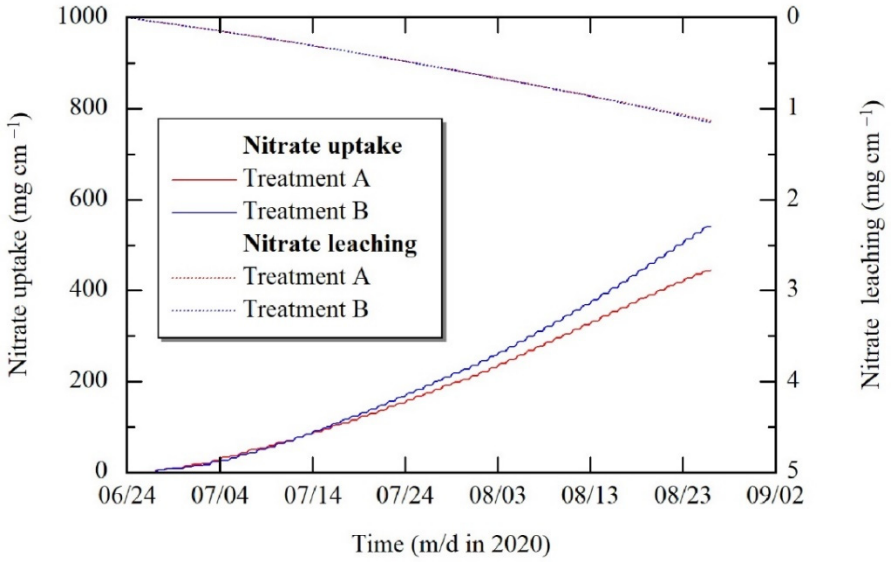


**Figure 8.** The fate of both nitrate uptake and leaching throughout the growing season. (Treatment A donates the proposed scheme, while treatment B donates the sensor-based irrigation method).

**Table 1.** Statistical analysis for maize yield components. Means in each column followed by "NS" indicates non-significant differences ($p \leq 0.05$) and ±SE indicates the standard error. (Treatment A and Treatment B refer to the proposed scheme and a sensor-based irrigation method, respectively).

| Plant Parameter | Treatment A | Treatment B |
|---|---|---|
| PH (cm) | $317 \pm 13.3^{NS}$ | $315 \pm 2.9$ |
| LAI | $5.3 \pm 0.3^{NS}$ | $5.0 \pm 0.2$ |
| Stem DM (g)/plant | $517 \pm 39^{NS}$ | $603 \pm 38$ |
| Leaves DM (g)/plant | $98 \pm 2.5^{NS}$ | $94 \pm 5.1$ |
| Ear weight (g)/plant | $418 \pm 21^{NS}$ | $418 \pm 24$ |
| Ear diameter (cm) | $4.51 \pm 0.08^{NS}$ | $4.52 \pm 0.13$ |
| Ear length (cm) | $21.6 \pm 1.08^{NS}$ | $22.3 \pm 1.36$ |
| Cob weight (g) | $46.6 \pm 4.7^{NS}$ | $48 \pm 5.86$ |
| Num. Lines/ear | $14 \pm 0.4^{NS}$ | $14 \pm 0.6$ |
| Num. kernels/ear | $40 \pm 2.3^{NS}$ | $39 \pm 2.8$ |
| Weight/plant (g) | $378 \pm 30^{NS}$ | $320 \pm 32$ |
| 100 kernels weight/ear (g) | $35.9 \pm 0.9^{NS}$ | $37.3 \pm 1.3$ |

The graph demonstrates the response of either observed soil VWC or simulated ones under five irrigation events. In comparison to the observed values, the model could accurately simulate VWC, when the sensor was placed at 5 cm below the emitter, with an RMSE of 0.02 $cm^3$ $cm^{-3}$. This result indicates that the model can simulate soil water flow with fairly good accuracy in the topsoil layer (5 cm according to the observation), where evaporation is active. We attempted to confirm the accuracy of the model in deeper soil layers, but placing a 5TE sensor 30 cm under the emitter caused extraordinary readings even after correction for the specific calibration function. Datta et al. [38] reported a similar observation in that none of five selected dielectric moisture sensors gave satisfactory readings under high levels of salinity and clay content, instead overestimating both the field capacity and wilting point. In general, large fluctuation occurs near the soil surface and if the change near the surface is accurately predicted, the model is expected to predict water content accurately in the deeper layer, too. Irrigation was applied for treatment B when 70% of available water was depleted, and the irrigation interval was decreased by the crop development as shown in Figure 11.

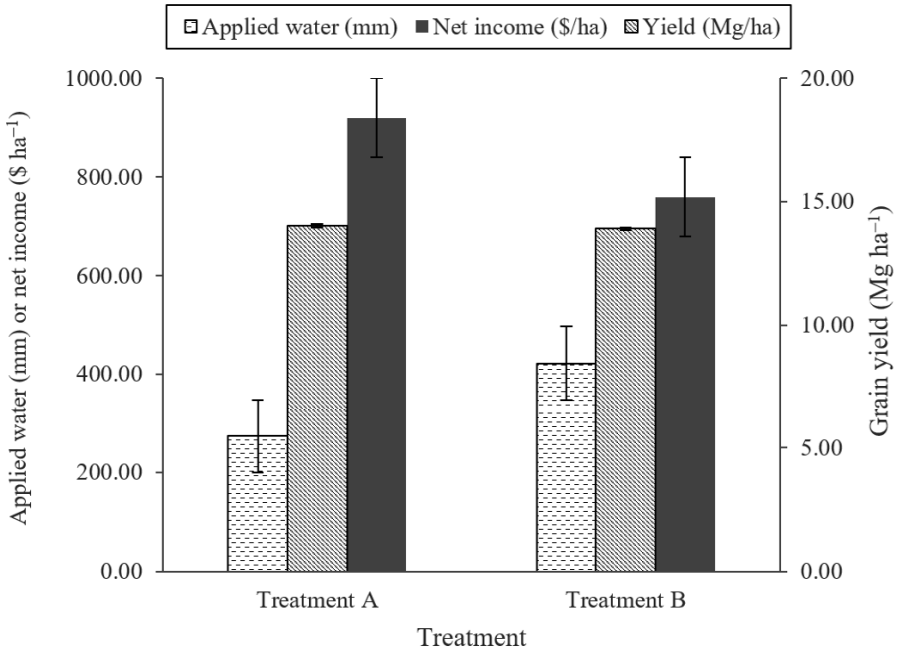


**Figure 9.** Comparison of net income, grain yield, and applied water between the two methods (treatment A refers to the proposed scheme, while treatment B refers to the sensor-based irrigation). Note that error bars represent the standard error.

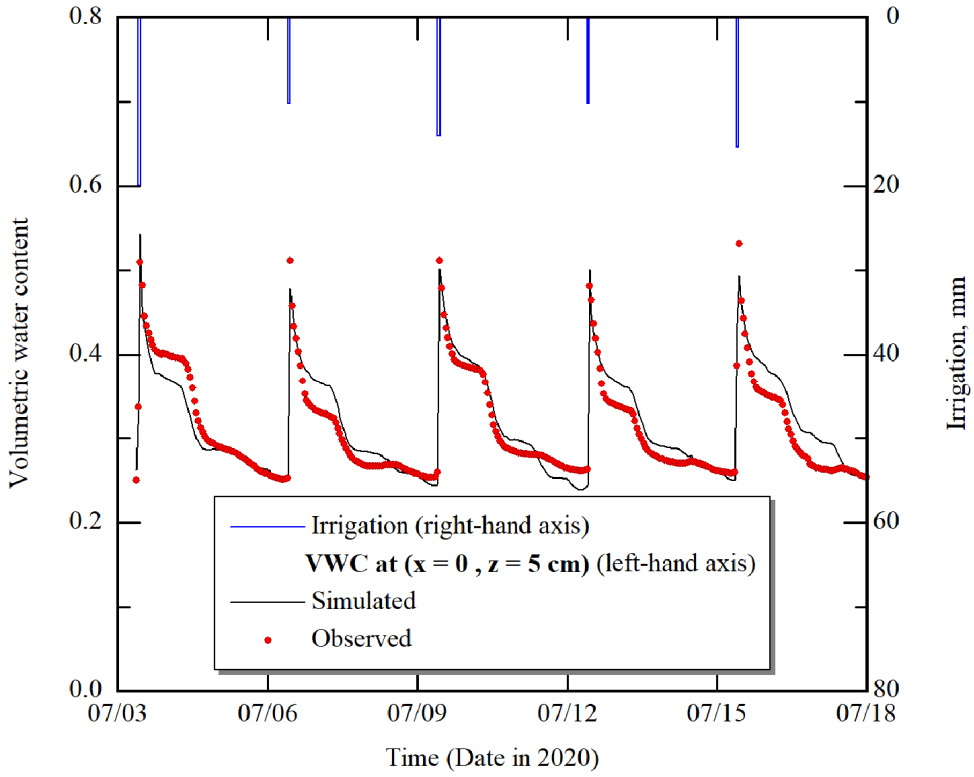


**Figure 10.** Comparison between simulated and observed VWC values with treatment A (x donates the horizontal distance from the drip tube while z is the soil depth).

### *3.4. An Example for Determining Irrigation Depth Using the Proposed Numerical Scheme*

An example for determining irrigation depth is illustrated in Figure 12. On 6 July, the model suggested an irrigation depth of 9.9 mm for three days to achieve a maximum net income of 24 \$ $ha^{-1}$. The optimum irrigation depth was determined from three points of *W*:

0, 20, and 40 mm by predicting another three points of $\tau_i$: 2.57, 6.1, and 6.1 mm, respectively. $\tau_i$ reached its maximum value at around $W$ = 20 mm, then it levelled-off. These results indicate the validity of the two-point scheme reported by Abd El Baki et al. [29], which assumes that $\tau_i$ is a linear function of $W$.

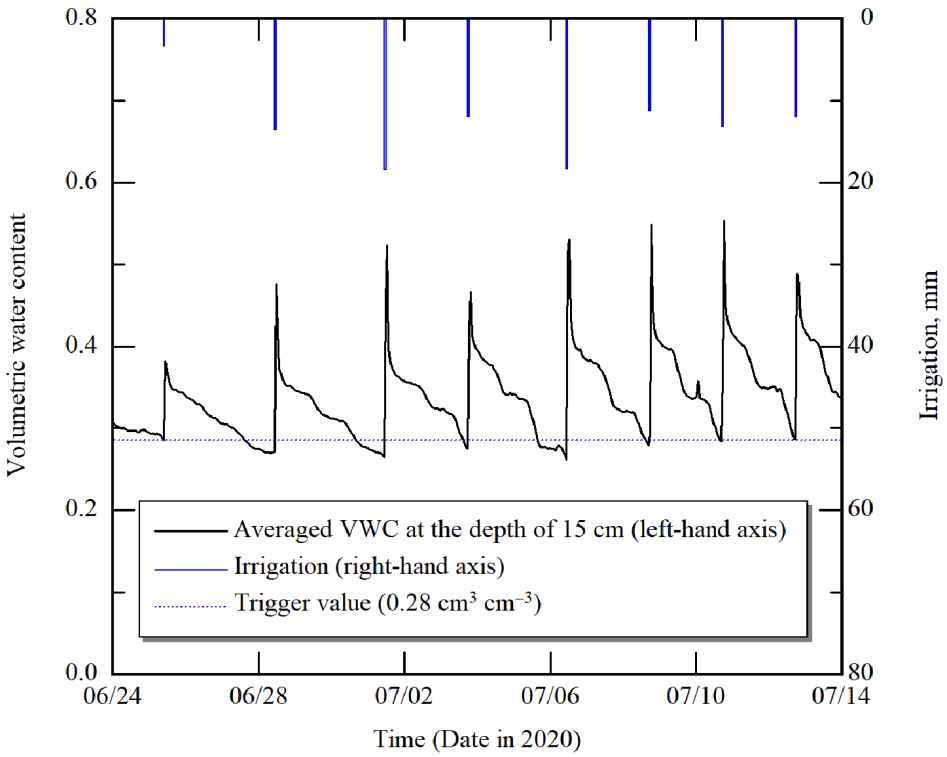


**Figure 11.** Fluctuation of VWC in response to irrigation events from 24 June to 14 July under treatment B.

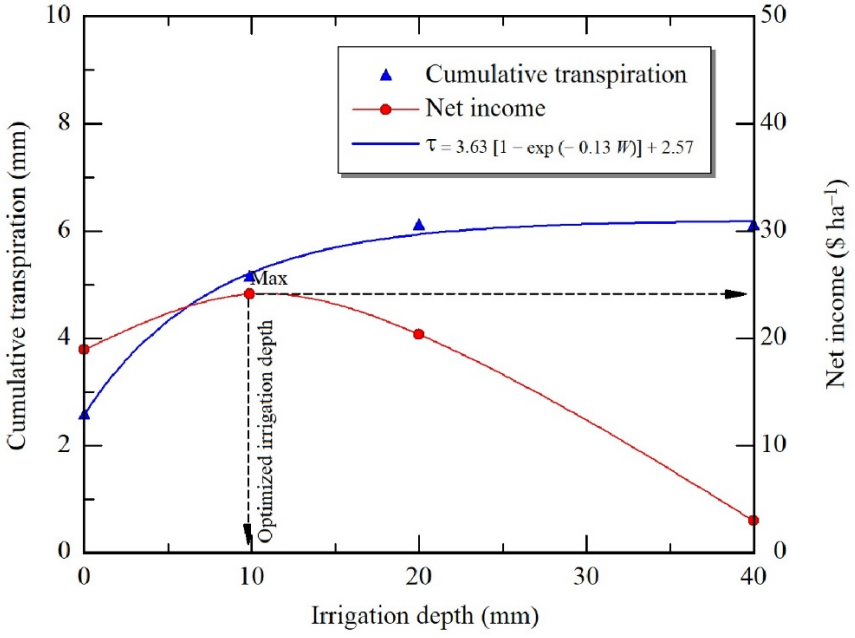


**Figure 12.** An optimization example to determine irrigation depth that maximizes net income on 06 July.

## 4. Conclusions

A field experiment was carried out in the Nile delta to evaluate the effectiveness of a new scheme to determine irrigation depth under the combination of dry climate and clay loamy soil. The scheme employed three predicted points of cumulative transpiration at each irrigation interval, a volumetric water price, and quantitative weather forecasts to maximize farmers' net income per unit of water use. Results indicate that the proposed scheme could increase net income and save water by 21% and 35%, respectively, compared with sensor-based irrigation. There were no significant differences in the grain yield production and the whole of the observed yield components, with similar standard error values in both methods, except for plant height, which was higher in the proposed scheme. This was one of the factors that contributed to the growth of non-grain biomass for the sensor-based irrigation scheme, despite having similar grain yield compared to the proposed scheme. The model could simulate water flow in the top 5 cm of the soil layer with an RSME 0.02 $cm^3$ $cm^{-3}$. The findings of this study indicate that the proposed scheme is applicable to the combination of dry climate and clay loamy soil and in parallel with previous studies conducted in sandy soil, the scheme has the potential to be a useful tool for reducing the initial costs of expensive monitoring sensors while improving irrigation management and net income.

**Author Contributions:** Conceptualization, H.F.; methodology, H.M.A.E.B. and H.F.; Software, H.F.; validation, H.M.A.E.B.; writing—original draft preparation, H.M.A.E.B.; writing—review and editing, H.F.; supervision, H.F.; project administration, H.F.; funding acquisition, H.F. Both authors have read and agreed to the published version of the manuscript.

**Funding:** This research was funded by the Ministry of Education, Culture, Sports Science and Technology (MEXT). The joint research project is being carried out by the Arid Land Research Center (ALRC), namely "Development of crop husbandry technology in rainfed marginal regions using dryland plant resources" (http://www.alrc.tottori-u.ac.jp/genkaichi/en/, accessed on 5 June 2021).

**Institutional Review Board Statement:** Not applicable.

**Informed Consent Statement:** Informed consent was obtained from all subjects involved in the study.

**Data Availability Statement:** The data is available on the request of the corresponding author.

**Acknowledgments:** We thank the landowner for his great support for the success of such a research.

**Conflicts of Interest:** The authors declare no conflict of interest. The funding sponsors had no role in the design of the study; in the collection, analyses, or interpretation of data; in the writing of the manuscript; or in the decision to publish the results.

## References

1. Amer, M.H.; Abd El Hafez, S.A.; Abd El Ghany, M.B. (Eds.) *Introduction. Water Saving in Irrigated Agriculture in Egypt*, 1st ed.; LAP LAMBERT Academic Publishing: Beau Bassin, Mauritius, 2017; p. 2. [CrossRef]
2. English, M. Deficit irrigation. I. Analytical framework. *J. Irrig. Drain E* **1990**, *116*, 399–412. [CrossRef]
3. Kirda, C. *Deficit Irrigation Scheduling Based on Plant Growth Stages Showing Water Stress Tolerance*; Deficit Irrigation Practices, Water Reports; Food and Agricultural Organization of the United Nations: Rome, Italy, 2002; Volume 22.
4. Abuhashim, M.; Negm, A.M. (Eds.) *Deficit Irrigation Management as Strategy under Conditions of Water Scarcity; Potential Application in North Sinai, Egypt. Sustainability of Agricultural Environment in Egypt: Part I-Soil-Water-Food Nexus*, 1st ed.; Springer: Cham, Switzerland, 2018; pp. 35–55. [CrossRef]
5. Comas, L.H.; Trout, T.J.; DeJonge, K.C.; Zhang, H.; Gleason, S.M. Water productivity under strategic growth stage-based deficit irrigation in maize. *Agric. Water Manag.* **2019**, *212*, 433–440. [CrossRef]
6. Li, X.; Zhao, W.; Jiang, H.; Li, J.; Li, Y. Maximizing water productivity of winter wheat by managing zones of variable rate irrigation at different deficit levels. *Agric. Water Manag.* **2019**, *216*, 153–163. [CrossRef]
7. Bell, J.M.; Schwartz, R.; McInnes, K.J.; Howell, T.; Morgan, C.L.S. Deficit irrigation effects on yield and yield components of grain sorghum. *Agric. Water Manag.* **2018**, *203*, 289–296. [CrossRef]

8. Fujimaki, H.; Tokumoto, I.; Saito, T.; Inoue, M.; Shibata, M.; Okazaki, T.; Nagaz, K.; El Mokh, F. Determination of irrigation depths using a numerical model and quantitative weather forecast and comparison with an experiment. In *Practical Applications of Agricultural System Models to Optimize the Use of Limited Water*; Ahuja, L.R., Ma, L., Lascano, R.J., Eds.; ACSESS: Madison, WI, USA, 2015; Volume 5, pp. 209–235. [CrossRef]
9. Romeroa, R.; Muriel, J.L.; García, I.; de la Pena, D.M. Research on automatic irrigation control: State of the art and recent results. *Agric. Water Manag.* **2012**, *114*, 59–66. [CrossRef]
10. Domínguez-Niño, J.M.; Oliver-Manera, J.; Girona, J.; Casadesús, J. Differential irrigation scheduling by an automated algorithm of water balance tuned by capacitance-type soil moisture sensors. *Agric. Water Manag.* **2020**, *228*, 105880. [CrossRef]
11. Sui, R.; Vories, E.D. Comparison of sensor-based and weather-based irrigation scheduling. *Appl. Eng. Agric.* **2020**, *36*, 375–386. [CrossRef]
12. Hedley, C.B.; Knox, J.W.; Raine, S.R.; Smith, R. Water: Advanced Irrigation Technologies. *Encycl. Agric. Food Syst.* **2014**, *5*, 378–406. [CrossRef]
13. Adeyemi, O.; Grove, I.; Peets, S.; Norton, T. Advanced Monitoring and Management Systems for Improving Sustainability in Precision Irrigation. *Sustainability* **2017**, *9*, 353. [CrossRef]
14. Li, J.; Jiao, X.; Jiang, H.; Song, J.; Chen, L. Optimization of Irrigation Scheduling for Maize in an Arid Oasis Based on Simulation–Optimization Model. *Agronomy* **2020**, *10*, 935. [CrossRef]
15. Pereira, L.S.; Paredes, P.; Jovanovic, N. Soil water balance models for determining crop water and irrigation requirements and irrigation scheduling focusing on the FAO56 method and the dual Kc approach. *Agric. Water Manag.* **2002**, *241*, 106357. [CrossRef]
16. Allen, R.; Pereira, L.; Raes, D.; Smith, M. *Crop Evapotranspiration: Guidelines for Computing Crop Water Requirements*; FAO Irrigation and Drainage Paper No. 56; FAO: Rome, Italy, 1998; pp. 135–142.
17. Šimunek, J.; van Genuchten, M.T.; Šejna, M. *The HYDRUS Software Package for Simulating Two- and Three-Dimensional Movement of Water, Heat, and Multiple Solutes in Variably-Saturated Media, Technical Manual, Version 1.0 p.*; Republic PC Progress: Prague, Czech Republic, 2006; p. 241. [CrossRef]
18. Selim, T.; Berndtsson, R.; Persson, M. Simulation of soil and salinity distribution under surface drip irrigation. *Irrig. Drain.* **2013**, *62*, 352–362. [CrossRef]
19. Noshadi, M.; Fahandej-Saadi, S.; Sepaskhah, A.R. Application of SALTMED and HYDRUS-1D models for simulations of soil water content and soil salinity in controlled groundwater depth. *J. Arid Land* **2020**, *12*, 447–461. [CrossRef]
20. Er-Raki, S.; Ezzahar, J.; Merlin, O.; Amazirh, A.; Ait Hssaine, B.; Kharrou, M.H.; Khabba, S.; Chehbouni, A. Performance of the HYDRUS-1D model for water balance components assessment of irrigated winter wheat under different water managements in semi-arid region of Morocco. *Agric. Water Manag.* **2021**, *244*, 106546. [CrossRef]
21. Lorite, I.J.; Ramírez-Cuesta, J.M.; Cruz-Blanco, M.; Santos, C. Using weather forecast data for irrigation scheduling under semi-arid conditions. *Irrig. Sci.* **2015**, *33*, 411–427. [CrossRef]
22. Wang, D.B.; Cai, X.M. Irrigation scheduling-role of weather forecasting and farmers' behavior. *J. Water Resour. Plan. Manage.* **2009**, *135*, 364–372. [CrossRef]
23. Linker, L.; Sylaios, G. Efficient model-based sub-optimal irrigation scheduling using imperfect weather forecasts. *J. Comput. Electron. Agric.* **2016**, *130*, 118–127. [CrossRef]
24. Jamal, A.; Linker, R.; Housh, M. Optimal Irrigation with Perfect Weekly Forecasts versus Imperfect Seasonal Forecasts. *J. Water Resour. Plan. Manag.* **2019**, *145*, 06019003. [CrossRef]
25. Abd El Baki, H.M.; Fujimaki, H.; Tokumoto, I.; Saito, T. Determination of irrigation depths using a numerical model of crop growth and quantitative weather forecast and evaluation of its effect through a field experiment for potato. *J. Jpn. Soc. Soil Phys.* **2017**, *136*, 15–24.
26. Abd El Baki, H.M.; Fujimaki, H.; Tokumoto, I.; Saito, T. A new scheme to optimize irrigation depth using a numerical model of crop response to irrigation and quantitative weather forecasts. *Comput. Electron. Agric.* **2018**, *150*, 387–393. [CrossRef]
27. Abd El Baki, H.M.; Fujimaki, H.; Tokumoto, I.; Saito, T. Optimizing Irrigation Depth Using a Plant Growth Model and Weather Forecast. *JAS* **2018**, *10*, 55–66. [CrossRef]
28. Abd El Baki, H.M.; Raoof, M.; Fujimaki, H. Determining Irrigation Depths for Soybean Using a Simulation Model of Water Flow and Plant Growth and Weather Forecasts. *Agronomy* **2020**, *10*, 369. [CrossRef]
29. Fujimaki, H.; Yanagawa, A. Application of Evaporation Method Using Two Tensiometers for Determining Unsaturated Hydraulic Conductivity beyond Tensiometric Range. *Eurasian Soil Sci.* **2019**, *52*, 405–413. [CrossRef]
30. Kubota, A.; Zayed, B.; Fujimaki, H.; Higashi, T.; Yoshida, S.; Mahmoud, M.M.A.; Kitamura, Y.; Abou El Hassan, W.H. *Water and Salt Movement in Soils of the Nile Delta. Irrigated Agriculture in Egypt*, 1st ed.; Satoh, M., Aboulroos, S., Eds.; Springer: Cham, Switzerland, 2017; pp. 153–186. [CrossRef]
31. TimeAndDate Website. Available online: https://www.timeanddate.com/weather/@352349/hourly (accessed on 5 September 2020).
32. Cai, J.; Liu, Y.; Lei, T.; Pereira, L.S. Estimating reference evapotranspiration with the FAO Penman–Monteith equation using daily weather forecast messages. *Agric. For. Meteorol.* **2007**, *145*, 22–35. [CrossRef]
33. El-Tantawy, M.M.; Ouda, S.A.; Khalil, F.A. Irrigation Scheduling for Maize Grown under Middle Egypt Conditions. Res. *J. Agric. Biol. Sci.* **2007**, *3*, 456–462.
34. Cornish, G.; Bosworth, B.; Perry, C. *Water Charging in Irrigated Agriculture—An Analysis of International Experience*; FAO: Rome, Italy, 2004; pp. 19–26. [CrossRef]

35. Infante, P.A.; Moore, K.; Hurburgh, C.; Scott, P.; Archontoulis, S.; Lenssen, A.; Fei, S. Biomass Production and Composition of Temperate and Tropical Maize in Central Iowa. *Agronomy* **2018**, *8*, 88. [CrossRef]
36. Satoh, M.; El Gamal, T.; Taniguchi, T.; Yuan, X.; Ishii, A.; Abou El Hassan, W.H. *Water Management in the Nile Delta. Irrigated Agriculture in Egypt*, 1st ed.; Satoh, M., Aboulroos, S., Eds.; Springer: Cham, Switzerland, 2017; pp. 187–224. [CrossRef]
37. Bozorg-Haddad, O.; Malmir, M.; Mohammad-Azari, S. Estimation of farmers' willingness to pay for water in the agricultural sector. *Agric. Water Manag.* **2016**, *177*, 284–290. [CrossRef]
38. Datta, S.; Taghvaeian, S.; Ochsner, T.E.; Moriasi, D.; Gowda, P.; Steiner, J.L. Performance Assessment of Five Different Soil Moisture Sensors under Irrigated Field Conditions in Oklahoma. *Sensors* **2018**, *18*, 3786. [CrossRef]